

Synthesis and Characterization of the Metalloplumbylenes $(\eta^5\text{-C}_5\text{H}_5)(\text{CO})_3\text{M-Pb-C}_6\text{H}_3\text{-2,6-Trip}_2$ (M = Cr, Mo, or W; Trip = $-\text{C}_6\text{H}_2\text{-2,4,6-i-Pr}_3$)

Lihung Pu,[†] Philip P. Power,^{*,†} Imke Boltes,[‡] and Regine Herbst-Irmer[‡]

Department of Chemistry, University of California, Davis, One Shields Avenue, Davis, California 95616, and Department of Structural Chemistry, University of Göttingen, Tammannstrasse 4, D-37077 Göttingen, Germany

Received October 1, 1999

The reaction of $\text{Pb}(\text{Br})\text{C}_6\text{H}_3\text{-2,6-Trip}_2$ (Trip = $\text{C}_6\text{H}_2\text{-2,4,6-i-Pr}_3$), generated in situ, with the salts $\text{Na}[\text{M}(\eta^5\text{-C}_5\text{H}_5)(\text{CO})_3]\cdot\text{DME}$ (M = Cr, Mo, or W; DME = 1,2-dimethoxyethane) affords the novel green, crystalline metalloplumbylenes $(\eta^5\text{-C}_5\text{H}_5)(\text{CO})_3\text{M-Pb-C}_6\text{H}_3\text{-2,6-Trip}_2$ (M = Cr, **1**; Mo, **2**; W, **3**) in moderate yield. The compounds were characterized spectroscopically (^1H , ^{13}C , and ^{207}Pb NMR, IR, and UV–vis) and by combustion analysis. In addition the X-ray crystal structures of **1–3** were determined. The compounds feature strongly bent geometries at lead (M–Pb–C = 108.6(2)–113.58(9)°) and relatively long M–Pb distances (2.9092(9) Å, Cr; 2.9845(7) Å, Mo; 2.9809(10) Å, 3.0055(6) Å W), which are consistent with single M–Pb bonding. The stability of the complexes, which melt with decomposition in the range 210–226 °C, is attributed to steric protection of the metal centers by the very large $-\text{C}_6\text{H}_3\text{-2,6-Trip}_2$ substituent. The compounds are the first examples of metalloplumbylenes that feature a bent two-coordinate lead geometry.

Introduction

Compounds that feature bonds between lead and the transition elements are less thoroughly investigated than their lighter group 14 element congeners.¹ Lower-valent lead derivatives are particularly rare and are confined to a handful of derivatives of various kinds.^{2,3} Examples include the spectroscopically characterized plumbylene complexes $(\text{CO})_5\text{MoPb}\{\text{CH}(\text{SiMe}_3)_2\}_2$ ⁴ and $[\text{Pd}(\eta^3\text{-C}_3\text{H}_5)(\mu\text{-Cl})\text{Pb}\{\text{N}(\text{SiMe}_3)_2\}_2]_2$ ⁵ as well as the structurally characterized bismetalloplumbylene derivatives $\{(\eta^5\text{-C}_5\text{H}_5)(\text{CO})_3\text{Mo}\}_2\text{Pb}\cdot\text{THF}$ and $\{(\eta^5\text{-C}_5\text{H}_5)(\text{CO})_3\text{Mo}\}_2\text{Pb}_2$ (dimerized through weak isocarbonyl interactions), both of which feature three-coordinate Pb(II) centers.⁶ In addition, the complex $[\text{NBu}_4]_2[\text{Pb}\{\text{Pt}(\text{C}_6\text{F}_5)_4\}_2]$,⁷ in which lead is bound linearly to two platinum, is thought to have single Pb–Pt bonds (Pt–Pb = ca. 2.78 Å), but there are eight Pt–F short contacts which may play a role in its stabilization. There are also related complexes such as $\text{Pb}\{\text{Mn}(\eta^5\text{-C}_5\text{H}_5)(\text{CO})_2\}_2$, which, how-

ever, are best regarded as consisting of Pb(IV) and two 18-electron $[\text{Mn}(\eta^5\text{-C}_5\text{H}_5)(\text{CO})_2]^{2-}$ moieties on the basis of their very short Pb–Mn bonds and linear coordination at the lead.⁸ Transition metal metalloplumbylenes featuring a bond between a two-coordinate uncomplexed lead(II) center, which bears a stereochemically active lone pair, and a transition metal moiety, e.g., of the type $\text{L}_n\text{M-Pb-R}$ (R = organo or related group, ML_n = transition metal fragment), are unknown at present. In fact, there are surprisingly few complexes of this type available for any of the heavier group 14 elements (Si–Pb). The only previously published examples are the spectroscopically characterized iron compounds $(\eta^5\text{-C}_5\text{R}_5)(\text{CO})_2\text{Fe-Ge-Mes}^*$ (R = H or Me; $\text{Mes}^* = \text{C}_6\text{H}_2\text{-2,4,6-t-Bu}_3$) and the closely related species $(\eta^5\text{-C}_5\text{H}_5)(\text{CO})_2\text{Fe-Ge-CH}(\text{SiMe}_3)_2$.⁹ In this paper it is shown that the use of a terphenyl ligand,¹⁰ $-\text{C}_6\text{H}_3\text{-2,6-Trip}_2$ (Trip = $\text{C}_6\text{H}_2\text{-2,4,6-i-Pr}_3$), as a large, sterically protecting group permits the synthesis and structural characterization of the series of compounds $(\eta^5\text{-C}_5\text{H}_5)(\text{CO})_2\text{M-Pb-C}_6\text{H}_3\text{-2,6-Trip}_2$ (M = Cr, Mo, or W), which are the first examples of stable metalloplumbylenes of this type.

Experimental Section

General Procedures. All manipulations were carried out by using modified Schlenk techniques under an atmosphere of N_2 or in a Vacuum Atmospheres HE-43 drybox. All solvents

[†] University of California, Davis.

[‡] University of Göttingen.

(1) Harrison, P. G. *Comprehensive Organometallic Chemistry*; Pergamon: Oxford, 1984; Vol. 2, Chapter 12. Harrison, P. G. *Comprehensive Organometallic Chemistry II*; Elsevier: Amsterdam, 1995; Vol. 2, Chapter 7.

(2) Kano, N.; Tokitoh, N.; Okazaki, R. *J. Synth. Org. Chem., Jpn.* **1998**, *56*, 11.

(3) Parr, J. *Polyhedron* **1997**, *16*, 551.

(4) Cotton, J. D.; Davidson, P. J.; Lappert, M. F. *J. Chem. Soc., Dalton Trans.* **1976**, 2275.

(5) Lappert, M. F.; Power, P. P. *J. Chem. Soc., Dalton Trans.* **1985**, 51.

(6) Hitchcock, P. B.; Lappert, M. F.; Michalczyk, M. J. *J. Chem. Soc., Dalton Trans.* **1987**, 2635.

(7) Usón, R.; Forníés, J.; Falvello, L. R.; Usón, M. A.; Usón, I. *Inorg. Chem.* **1992**, *31*, 369.

(8) Herrmann, W. A.; Kneuper, H.-J.; Herdtweck, E. *Angew. Chem., Int. Ed. Engl.* **1985**, *24*, 1062.

(9) Jutzi, P.; Leue, L. *Organometallics* **1994**, *13*, 2898.

(10) Twamley, B. T.; Haubrich, S. T.; Power, P. P. *Adv. Organomet. Chem.* **1999**, *44*, 1.

Table 1. Selected Crystallographic Data for Compounds 1–3

	1	2	3a	3b
formula	C ₄₄ H ₅₄ CrO ₃ Pb	C ₄₄ H ₅₄ MoO ₃ Pb	C ₄₄ H ₅₄ WO ₃ Pb	C ₄₄ H ₅₄ WO ₃ Pb
fw	890.06	934.00	1021.91	1021.91
cryst color/habit	green/parallelepiped	green/parallelepiped	green/parallelepiped	green/parallelepiped
cryst syst	monoclinic	monoclinic	monoclinic	monoclinic
space group	<i>P</i> 2 ₁ / <i>n</i>	<i>P</i> 2 ₁ / <i>n</i>	<i>P</i> 2 ₁ / <i>c</i>	<i>P</i> 2 ₁ / <i>n</i>
<i>a</i> (Å)	8.731(2)	13.156(2)	19.808(4)	13.178(2)
<i>b</i> (Å)	25.842(5)	20.606(3)	10.533(2)	20.701(3)
<i>c</i> (Å)	17.706(4)	15.129(2)	19.328(4)	15.151(2)
β (deg)	95.27(3)	102.91(2)	90.05(3)	102.94(2)
<i>V</i> (Å ³)	3978.1(15)	3997.7(10)	4032.5(14)	4028.2(10)
<i>Z</i>	4	4	4	4
cryst dimens, mm	0.4 × 0.3 × 0.1	0.4 × 0.2 × 0.1	0.3 × 0.3 × 0.2	0.4 × 0.2 × 0.2
<i>d</i> _{calc} (Mg m ^{−3})	1.486	1.552	1.683	1.685
μ (mm ^{−1})	4.537	4.556	7.056	7.064
2θ _{max} , deg	50	50	50	51.6
total no. of rflns	50921	55290	47364	49616
no. of unique rflns	7032	7056	7029	7716
<i>R</i> (int)	0.0873	0.1076	0.0917	0.0857
no. of obs rflns (<i>I</i> > 2(<i>σ</i>))	5435	5154	5279	6460
no. of params	582	455	591	454
no. of restraints	964	0	994	0
<i>R</i> 1(obsd)	0.0312	0.0367	0.0488	0.0544
w <i>R</i> 2(all data)	0.0755	0.0811	0.1060	0.1228
extinction coeff	0.00126(9)	0.00070(8)	0.00107(8)	
resid electron density, e Å ^{−3}	1.695/ −0.777	0.907/ −0.832	3.014/ −1.745	2.914/ −2.276

were distilled from Na/K alloy and degassed twice before use. The compounds Et₂O·Li(C₆H₃-2,6-Trip₂)¹¹ and Na[M(η⁵-C₅H₅)(CO)₃]·2DME (M = Cr, Mo, W)¹² were prepared according to literature procedures. PbBr₂ was purchased commercially and was used as received. ¹H, ¹³C, and ²⁰⁷Pb NMR spectroscopic data were recorded on a Bruker QE-300 spectrometer and referenced to the deuterated solvent. Infrared data were recorded on a Perkin PE-1430 instrument in the range 4000–200 cm^{−1} as Nujol mulls. UV–vis data were recorded on a Hitachi-1200 spectrometer. All compounds gave satisfactory C and H analyses.

(η⁵-C₅H₅)(CO)₃CrPbC₆H₃-2,6-Trip₂ (**1**). Pb(Br){C₆H₃-2,6-Trip₂} (ca. 2.26 mmol, prepared in situ from PbBr₂ (0.83 g) and Et₂O·LiC₆H₃-2,6-Trip₂ (1.27 g)) in toluene (20 mL) was added to Na[Cr(CO)₃(η⁵-C₅H₅)]·2DME (0.90 g, 2.23 mmol) in toluene (10 mL) at ca. −78 °C with constant stirring. The reaction mixture, which had assumed a green color, was stirred at ca. −78 °C for 30 min and for a further 4 h upon warming to room temperature. The toluene was removed under reduced pressure, and the greenish-blue residue was extracted with hexane (30 mL). After filtering through Celite, the volume of greenish-blue solution was reduced to incipient crystallization and stored in a ca. −20 °C freezer for 20 h to give product **1** as green crystals. Yield: 1.01 g, 50.8%. Mp: 218–226 °C dec. ¹H NMR (C₆D₆): δ = 1.10 (d, 12H, *p*-CH(CH₃)₂), ³*J*_{HH} = 6.0 Hz, 1.19 (d, 12H, *o*-CH(CH₃)₂), ³*J*_{HH} = 6.9 Hz, 1.44 (d, 12H, *o*-CH(CH₃)₂), ³*J*_{HH} = 6.9 Hz, 2.75 (sept, 2H, *p*-CH(CH₃)₂), ³*J*_{HH} = 6.9 Hz, 3.43 (broad, 4H, *o*-CH(CH₃)₂); 3.55 (s, η⁵-C₅H₅); 7.15 (s, 4H, *m*-Trip); 7.50 (t, 1H, *p*-C₆H₃), ³*J*_{HH} = 7.5 Hz, 8.07 (d, 2H, *m*-C₆H₃), ³*J*_{HH} = 7.5 Hz. ¹³C{H} (C₆D₆): δ 23.27 (*o*-CH(CH₃)₂), 24.13 (*o*-CH(CH₃)₂), 27.23 (*p*-CH(CH₃)₂), 30.77 (*o*-CH(CH₃)₂), 34.80 (*p*-CH(CH₃)₂), 87.55 (η⁵-C₅H₅), 121.96 (*m*-Trip), 125.13 (*p*-C₆H₃), 139.67 (*m*-C₆H₃), 133.88 (*i*-Trip), 145.63 (*p*-Trip), 147.55 (*o*-Trip), 149.41 (*o*-C₆H₃), 228.0 (br, CO). ²⁰⁷Pb NMR (C₆D₆): δ = 9563. IR (cm^{−1}): 1950(s), 1885(m), 1855(s). UV–vis (hexane): 624 nm (2100). Anal Calcd for C₄₄H₅₄CrO₃Pb: C, 59.73; H, 6.12. Found: C, 59.21; H, 6.30.

(η⁵-C₅H₅)(CO)₃MoPbC₆H₃-2,6-Trip₂ (**2**). Pb(Br){C₆H₃-2,6-Trip₂} (ca. 1.93 mmol, generated in situ from PbBr₂ (0.71 g) and Et₂O·LiC₆H₃-2,6-Trip₂ (1.09 g)) in toluene (25 mL) was added to Na[Mo(η⁵-C₅H₅)(CO)₃]·2DME (0.90 g, 2.0 mmol) in

toluene (10 mL) at ca. −78 °C with constant stirring. The reaction mixture was worked up in a manner similar to **1**, and the product **2** was isolated as blue-green crystals. Yield: 1.21 g, 67.2%. Mp: 219–221 °C dec. ¹H NMR (C₆D₆): δ = 1.11 (broad, 12H, *o*-CH(CH₃)₂), 1.21 (d, 12H, *o*-CH(CH₃)₂), ³*J*_{HH} = 6.9 Hz, 1.44 (d, 12H, *p*-CH(CH₃)₂), ³*J*_{HH} = 6.9 Hz, 2.77 (sept, 2H, *p*-CH(CH₃)₂), ³*J*_{HH} = 6.9 Hz, 3.46 (broad, 4H, *o*-CH(CH₃)₂), 4.05 (s, η⁵-C₅H₅), 7.15 (s, 4H, *m*-Trip), 7.55 (t, 1H, *p*-C₆H₃), ³*J*_{HH} = 7.5 Hz, 8.05 (d, 2H, *m*-C₆H₃), ³*J*_{HH} = 7.5 Hz. ¹³C{H} (C₆D₆): δ = 23.86 (*o*-CH(CH₃)₂), 24.04 (*o*-CH(CH₃)₂), 27.11 (*p*-CH(CH₃)₂), 30.75 (*o*-CH(CH₃)₂), 34.74 (*p*-CH(CH₃)₂), 91.81 (η⁵-C₅H₅), 122.01 (*m*-Trip), 125.06 (*p*-C₆H₃), 139.89 (*m*-C₆H₃), 133.67 (*i*-Trip), 145.83 (*p*-Trip), 147.51 (*o*-Trip), 149.23 (*o*-C₆H₃), 223.7 (br, CO). ²⁰⁷Pb NMR (C₆D₆): δ = 9659. IR (cm^{−1}): 1962(s), 1940(w,sh), 1890(m), 1865(s), 1830(w,sh). UV–vis (hexane): λ_{max} 616 nm (3700). Anal. Calcd for C₄₄H₅₄MoO₃Pb: C, 56.58; H, 5.83. Found: C, 57.10; H, 6.07.

(η⁵-C₅H₅)(CO)₃WPbC₆H₃-2,6-Trip₂ (**3**). Pb(Br){C₆H₃-2,6-Trip₂} (ca. 2 mmol, generated in situ from PbBr₂ (0.734 g) and Et₂O·LiC₆H₃-2,6-Trip₂ (1.13 g)) in toluene (25 mL) was added to Na[W(η⁵-C₅H₅)(CO)₃]·2DME (1.10 g, 2.05 mmol) in toluene (10 mL) at ca. 0 °C with constant stirring. The reaction mixture immediately became a blue-green color, and it was worked up in a manner similar to that of **1** to give the product **3** as green crystals. Yield: 0.98 g, 48%. Mp: 210–212 °C dec. ¹H NMR (C₆D₆): δ = 1.13 (broad, 12H, *o*-CH(CH₃)₂), 1.21 (d, 12H, *o*-CH(CH₃)₂), ³*J*_{HH} = 6.9 Hz; 1.45 (d, 12H, *p*-CH(CH₃)₂), ³*J*_{HH} = 6.9 Hz; 3.51 (broad, 4H, *o*-CH(CH₃)₂), 4.07 (s, η⁵-C₅H₅), 7.15 (s, 4H, *m*-Trip); 7.54 (t, 1H, *p*-C₆H₃), ³*J*_{HH} = 7.5 Hz; 8.02 (d, 2H, *m*-C₆H₃), ³*J*_{HH} = 7.5 Hz. ¹³C{H} (C₆D₆): δ = 23.56 (*o*-CH(CH₃)₂), 24.07 (*o*-CH(CH₃)₂), 27.14 (*p*-CH(CH₃)₂), 30.81 (*o*-CH(CH₃)₂), 34.78 (*p*-CH(CH₃)₂), 90.03 (η⁵-C₅H₅), 121.96 (*m*-Trip), 125.05 (*m*-C₆H₃), 133.86 (*i*-Trip), 139.51 (*p*-C₆H₃), 145.73 (*p*-Trip), 147.56 (*o*-Trip), 149.11 (*o*-C₆H₃), 211.75 (CO) (J_{C,w} = 86 Hz). ²⁰⁷Pb NMR (C₆D₆): δ = 9374. IR (cm^{−1}): 1953(s), 1930(m,sh), 1878(m), 1851(s), 1825(w,sh). UV–vis (hexane): λ_{max} 611 nm (2700). Anal. Calcd for C₄₄H₅₄O₃PbW: C, 51.71; H, 5.33. Found: C, 52.18; H, 5.48.

X-ray Data Collection and Refinement. Crystal data are summarized in Table 1. Data were collected at −140 °C on a Stoe-Siemens-Huber four-circle diffractometer equipped with a Siemens SMART area detector. Monochromated Mo Kα radiation (λ = 0.71073 Å) was used. A semiempirical absorption correction using equivalents was employed. The structures

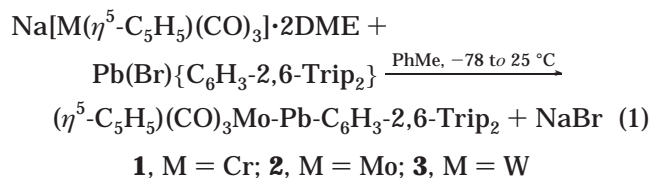
(11) Schiemenz, B.; Power, P. P. *Organometallics* **1996**, *15*, 958.

(12) Braunstein, P.; Bender, R.; Jud, J. *Inorg. Synth.* **1989**, *26*, 341.

were solved by direct methods.¹³ All non-hydrogen atoms were refined anisotropically.¹⁴ For the hydrogen atoms the riding model was used. The structures were refined against F^2 with a weighting scheme of $w^{-1} = \sigma^2(F_o^2) + (g_1P)^2 + g_2P$ with $P = (F_o^2 + 2F_c^2)/3$. The R values are defined as $R1 = \sum ||F_o| - |F_c|| / \sum |F_o|$ and $wR2 = [\sum w(F_o^2 - F_c^2)^2 / \sum wF_o^4]^{0.5}$. For structure **3** two data collections were obtained owing to the poor quality of the first crystal. The cell parameters of the second sample are different. Therefore we provide data for two crystal structures of the W compound (**3a** and **3b**). In structures **1** and **3a** one of the Trip groups is disordered. They were refined with distance restraints and restraints for the anisotropic replacement parameters. Anomalous electron densities were observed in the neighborhood of tungsten in both **3a** and **3b** which were attributed to uncorrected absorption effects.

Results and Discussion

Synthesis. The compounds **1–3** were synthesized in a straightforward manner by the reaction of 1 equiv of $\text{Pb}(\text{Br})\text{C}_6\text{H}_3\text{-2,6-Trip}_2$ (which was generated in situ from PbBr_2 and $\text{Et}_2\text{O}\cdot\text{LiC}_6\text{H}_3\text{-2,6-Trip}_2$), with the sodium salts $\text{Na}[\text{M}(\eta^5\text{-C}_5\text{H}_5)(\text{CO})_3]\cdot 2\text{DME}$ ($\text{M} = \text{Cr}, \text{Mo}, \text{or W}$).



The reaction proceeded smoothly, and in moderate yield, to afford the products as green, air-sensitive crystals which decompose with CO evolution at relatively high temperatures. However, hydrocarbon solutions of **1–3** decompose slowly at room temperature over 2–3 days to afford a lead mirror and various decomposition products. Nonetheless, the stability of the compounds **1–3** may be contrasted with the product of the corresponding reaction of $\text{Na}[\text{Mo}(\eta^5\text{-C}_5\text{H}_5)(\text{CO})_3]$ with $\text{Ge}(\text{Cl})\text{-C}_6\text{H}_3\text{-2,6-Mes}_2$ ($\text{Mes} = \text{C}_6\text{H}_2\text{-2,4,6-Me}_3$), which resulted in the triply bonded species $(\eta^5\text{-C}_5\text{H}_5)(\text{CO})_2\text{Mo}\equiv\text{Ge-C}_6\text{H}_3\text{-2,6-Mes}_2$ with CO elimination under ambient conditions.¹⁵ The greater difficulty in forming a species with a triply bonded lead atom may be a consequence of the greater relative stability ("inert pair" effect) of the $\text{Pb}(\text{II})$ lone pair as well as the larger size of lead, which decreases the amount of steric congestion and makes CO elimination less likely.

Structures. The structures of **1–3** were determined by X-ray crystallography, and they may be illustrated by the thermal ellipsoid plot of **2** in Figure 1. All compounds have very similar structures, as shown by the selected structural data in Table 2. Indeed, crystals of **2** and the second structure of **3** (i.e., **3b**) are isomorphous. The crystals **3a** and **3b** differ only in the crystal packing, and their bond lengths and angles are nearly identical. The main features of interest of all the structures concern the metal–lead distances and the interligand angle at lead. The long M–Pb bond lengths, together with the bent geometries at lead in **1–3**, and the presence of three carbonyl ligands in each complex demonstrate the existence of a stereochemically active

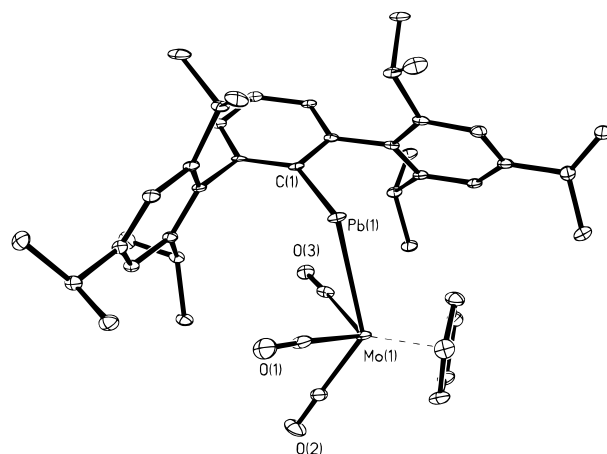


Figure 1. Computer-generated thermal ellipsoidal (50% drawing of **2** illustrating the bent geometry at lead. Hydrogen atoms are not shown for clarity. Important bond distances and angles for this compound and its chromium and tungsten analogues (**1**, **3a**, and **3b**) are given in Table 2.

Table 2. Selected Bond Distances (Å) and Angles (deg) for **1–3**

	1 ($\text{M} = \text{Cr}$)	2 ($\text{M} = \text{Mo}$)	3a ($\text{M} = \text{W}$)	3b ($\text{M} = \text{W}$)
Pb–C	2.294(4)	2.291(5)	2.283(7)	2.278(9)
Pb–Cr	2.9092(9)	2.9845(7)	2.9809(10)	3.0055(6)
M–C(CO) (av)	1.837(8)	1.963(5)	1.961(11)	1.973(11)
M–C($\eta^5\text{-C}_5\text{H}_5$)	2.182(5)	2.335(6)	2.332(8)	2.314(13)
	2.183(5)	2.338(6)	2.344(9)	2.326(10)
	2.195(5)	2.354(7)	2.347(9)	2.355(9)
	2.197(5)	2.357(6)	2.361(10)	2.357(10)
	2.198(5)	2.371(7)	2.379(9)	2.359(11)
C–O (av)	1.158(2)	1.156(7)	1.156(8)	1.162(13)
M–Pb–C	113.58(9)	110.00(13)	108.6(2)	109.36(19)
OC–M–CO	81.9(2)	78.9(3)	76.1(4)	79.2(4)
	82.1(2)	82.8(3)	84.8(5)	83.0(4)
	105.0(2)	101.3(3)	100.4(4)	101.5(4)
Pb–C–C	112.8(3)	118.1(4)	116.4(5)	118.3(6)
	124.5(3)	120.2(4)	121.4(6)	121.3(6)

lone pair and a single M–Pb bond between the 17-electron $\text{M}(\eta^5\text{-C}_5\text{H}_5)(\text{CO})_3$ fragment and the PbAr moiety. The Cr–Pb bond length, 2.9092(9) Å, in **1** may be compared with the significantly shorter distances of 2.658(2) Å in $\text{bipyPb}\{\text{Cr}(\text{CO})_5\}_2$ ¹⁶ ($\text{bipy} = \text{bipyridyl}$) and the average distance of 2.724(2) Å in the dianion $[\{\text{Me}(\text{O})\text{CO}\}_2\text{Pb}\{\text{Cr}(\text{CO})_5\}_2]^{2-}$.¹⁷ The short Cr–Pb bond in the bipy complex could be due to the fact that the formal oxidation state of lead is 4+ (assuming the transition metal fragment is $[\text{Cr}(\text{CO})_5]^{2-}$) and that there is some multiple character in the Cr–Pb bond ($\text{Cr–Pb–Cr} = 155.47(8)^\circ$). In addition, the effective coordination number of chromium, both in this compound and the dianion $[\{\text{Me}(\text{O})\text{CO}\}_2\text{Pb}\{\text{Cr}(\text{CO})_5\}_2]^{2-}$, is six,¹⁵ whereas in **1** it is seven. The long Cr–Pb bond distances (range 2.88(1)–2.99(1) Å seen in the cluster anion $[(\text{CO})_3\text{-CrPb}_9]^{4-}$,¹⁸ which also contains a formally seven-coordinate chromium (bound to three carbonyl ligands and four lead atoms), seem to support the influence of the chromium coordination number on the Cr–Pb bond length.

(16) Kircher, P.; Huttner, G.; Heinze, K.; Schiemenz, B.; Zsolnai, L.; Büchner, M.; Driess, A. *Eur. J. Inorg. Chem.* **1998**, 703.

(17) Kircher, P.; Huttner, G.; Schiemenz, B.; Heinze, K.; Zsolnai, L.; Walter, O.; Jacobi, A.; Driess, A. *Chem. Ber.* **1997**, 130, 687.

(18) Eichorn, B.; Haushalter, R. C. *J. Chem. Soc., Chem. Commun.* **1990**, 937.

(13) Sheldrick, G. M. *Acta Crystallogr.* **1990**, A46, 467.

(14) Sheldrick, G. M. *SHELXL-97*, University of Göttingen, 1997.

(15) Simons, R. S.; Power, P. P. *J. Am. Chem. Soc.* **1996**, 118, 11966.

The major difference between the structure of **1** and those of **2** and **3** concerns the metal–ligand distances. The Mo–Pb and W–Pb bond lengths, 2.9845(7) (**2**), 2.9809(10) (**3a**), and 3.0055(6) Å (**3b**), are very similar and are 0.075, 0.072, and 0.096 Å longer than the corresponding Cr–Pb distance. A bond length increase is predicted in view of the larger sizes of molybdenum and tungsten atoms (metallic radii: Cr = 1.29 Å; Mo = 1.40 Å; W = 1.41 Å).¹⁹ However, the differences in metallic radii between chromium and molybdenum or tungsten (0.11 and 0.12 Å) are somewhat greater than the differences in M–Pb bond lengths between **1** and **2** or **3**. In contrast, there is a ca. 0.12 Å difference between the Cr–C(CO) distances and the corresponding M–C bonds in the molybdenum and tungsten complexes. In addition it is notable that the sum of the single-bonded metallic radius of lead (1.54 Å)²⁰ and the transition metal radii affords predicted bond lengths 2.83, 2.95, and 2.96 Å for the Cr–Mo or W–Pb bonds. Thus the metal–metal bonds in **1–3** are invariably longer than the predicted values.

The differences between the predicted and measured M–Pb bond lengths for **1–3** are also seen to an even greater degree in some related complexes. For example, Mo–Pb and W–Pb distances of 2.808(1) and 2.766(2) Å have been reported for the complexes {Me(O)CO}₂Pb–{Mo(H)(η^5 -C₅H₅)₂}₂²¹ and (η^5 -C₅H₅)W(SnPh₃){Pb(Cl)-Me₂}.²² These are ca. 0.2 Å shorter than the corresponding distances in **2** or **3**. However, the bismetalloplumbylenes {(η^5 -C₅H₅)(CO)₃Mo}₂Pb·THF and [{(η^5 -C₅H₅)(CO)₃-Mo}₂Pb]₂ have Pb–Mo distances in the range 2.989(2)–3.019(2) Å,⁶ which are very close to the values in **2** and **3**. These complexes also feature lead(II), which has a three-coordinate pyramidal geometry through further complexation either to a THF or to an oxygen from a carbonyl in a neighboring molecule. Although at present the number of structures is small, it is clear that, in the absence of multiple bonding, the lower oxidation state lead(II) species display substantially longer bond lengths to transition metals than their Pb(IV) counterparts. The relatively long lead carbon distances of ca. 2.29 Å in **1–3** also support this view since they are closer to the values observed in the plumbylenes Pb(C₆H₃-2,6-Mes₂)₂ (Pb–C = 2.334(12) Å),²³ Pb(Tbt)₂ (Pb–C = 2.327(13) Å, Tbt = C₆H₂-2,4,6-{CH(SiMe₃)₂})₃,²⁴ and Pb(C₆H₂-2,4,6-t-Bu₃)(CH₂CMe₂C₆H₃-3,5-t-Bu₂)[Pb–C(Ar) = 2.344(9) Å]²⁵ than they are to the shorter Pb–C distances of ca. 2.22 Å in many tetravalent lead species such as Ph₃PbPbPh₃²⁶ and (η^5 -C₅H₅)₂W(SnPh₃){Pb(Cl)-Me₂}.²² The relatively short Pb–Pb bond length of 2.844(4) Å, observed in the structure of Ph₃PbPbPh₃, is fully consistent with these results, although it appears

that several other factors also influence bond lengths in organolead compounds.²⁷

The transition metal–carbon distances to the η^5 -C₅H₅ and CO ligands in **1–3** are in the normal range. For example the average Cr–C(η^5 -C₅H₅) distance in **1** is 2.191(7) Å, which is very close to the 2.20 Å in the dimer [Cr(η^5 -C₅H₅)(CO)₃]₂,²⁸ while the average Cr–C(CO) bond length, 1.837(8) Å, is slightly shorter than the average value of 1.86(1) Å in [Cr(η^5 -C₅H₅)(CO)₃]₂. The corresponding distances in **2** and **3** are generally within 0.02 Å of these in the dimers [M(η^5 -C₅H₅)(CO)₃]₂ (M = Mo²⁹ or W²⁹). It can be seen from the data in Table 2 that the C–O bond lengths (average 1.157(2) Å) are almost identical in the three lead derivatives. The interligand angles at lead in **1–3** are in the range 108.6(2)–113.58(9)°. These angles are somewhat narrower than the 114.5(6)° and 116.3(7)° observed in Pb(C₆H₃-2,6-Mes₂)₂²³ or Pb(Tbt)₂²⁴ but significantly wider than the 94.5(1)° in Pb{C₆H₂-2,4,6-(CF₃)₃}₃.³⁰ In these compounds at least, it seems probable that it is the steric bulk of the substituents that plays the primary role in governing the interligand angle at lead.

Spectroscopy. The ¹H, ¹³C, and ²⁰⁷Pb NMR spectra of **1–3** are of considerable use in establishing the purity of the samples as well as their solution structures. The ¹H NMR spectra displayed peaks attributable to the –C₆H₃-2,6-Trip₂ and η^5 -C₅H₅ moieties in a 1:1 ratio. In the ¹³C{¹H} NMR spectrum of each compound the peak due to carbonyl groups was broad, possibly as a result of the existence of restricted rotation around the group 6 metal–lead bond similar to that seen in the ¹³C NMR spectra of [M(η^5 -C₅H₅)(CO)₃]₂ (M = Mo or W)³¹ dimers. We were unable to assign resonances for Pb–C(ipso) carbons, however. The ²⁰⁷Pb NMR spectra of **1–3** displayed single broad peaks in the range 9374–9563 ppm. These low-field chemical shifts are undoubtedly due to the low coordination number of the lead atom in each case and are consistent with the values reported for Pb(Tbt)₂ (δ = 9751) and various plumbylenes.²⁴

The infrared spectra of the metalloplumbylenes **1–3** bear a close resemblance to each other in the CO stretching region. Each compound features three major bands in the ranges 1950–1962, 1878–1890, and 1851–1865 cm^{−1}, which also contain shoulder features. These are similar to the frequencies found in related species. For example the CO stretching frequencies in the complex {(η^5 -C₅H₅)(CO)₃Mo}₂Pb·THF⁶ at 1974(s), 1940(s), 1889(s), 1860(s), and 1846(s) cm^{−1} are marginally (0–12 cm^{−1}) higher than the corresponding ones in **2**. The major feature in the UV–vis spectra of **1–3** is an absorption at 624 (**1**), 616 (**2**), or 611 (**3**) nm, which can be assigned to the lead n–p electronic transitions. These peaks are red shifted in comparison to the absorption at 526 nm observed for the monomeric diaryllead compound Pb(C₆H₃-2,6-Mes₂)₂,²³ which has a C–Pb–C angle of 114.5(6)°. However, they are very close to the

(19) Wells, A. F. *Structural Inorganic Chemistry*, 5th ed.; Clarendon, Oxford, 1984; p 1298.

(20) Pauling, L. *The Nature of the Chemical Bond*, 3rd ed.; Cornell: Ithaca, 1960; p 257.

(21) Kubick, M. M.; Kergoat, R.; Guerschais, J.-E.; L'Haridon, P. *J. Chem. Soc., Dalton Trans.* **1984**, 1791.

(22) Seebald, S.; Kickelbick, G.; Moller, F.; Schubert, U. *Chem. Ber.* **1996**, *129*, 1131.

(23) Simons, R. S.; Pu, L.; Olmstead, M. M.; Power, P. P. *Organometallics* **1997**, *16*, 1920.

(24) Kano, K.; Shibata, K.; Tokitoh, N.; Okazaki, R. *Organometallics* **1999**, *18*, 2999.

(25) Stürmann, M.; Weidenbruch, M.; Klinkhammer, K. W.; Lissner, F.; Marsmann, H. *Organometallics* **1998**, *17*, 4425.

(26) Preut, H.; Hüber, F. Z. *Anorg. Allg. Chem.* **1976**, *419*, 92.

(27) Kaupp, M.; Schleyer, P. v. R. *J. Am. Chem. Soc.* **1993**, *115*, 1061.

(28) Adams, R. D.; Collins, D. E.; Cotton, F. A. *J. Am. Chem. Soc.* **1974**, *96*, 749.

(29) Adams, R. D.; Collins, D. M.; Cotton, F. A. *Inorg. Chem.* **1974**, *13*, 1086.

(30) Brooker, S.; Buijink, H.-K.; Edelmann, F. T. *Organometallics* **1991**, *10*, 25.

(31) (a) Todd, L. J.; Wilkinson, G. *J. Organomet. Chem.* **1974**, *77*,

1. (b) Lindsell, W. E.; Tomb, P. J. *J. Organomet. Chem.* **1989**, *378*, 245.

610 nm absorption observed for $\text{Pb}(\text{Tbt})_2$ ²⁴ or $\text{Pb}(\text{C}_6\text{H}_2\text{-t-Bu-4,5,6-Me}_3\text{)}\{\text{Si}(\text{SiMe}_3)_3\}$.²⁵ Apparently, the red shifts observed for **1–3** cannot be correlated with the interligand angle at lead, where the narrower interligand angle might have been expected to lead to a greater n–p energy separation.

Acknowledgment. We are grateful to the National Science Foundation for financial support.

Supporting Information Available: Tables giving full details of the crystallographic data and data collection parameters, atom coordinates, bond distances, bond angles, anisotropic thermal parameters, and hydrogen coordinates. This material is available free of charge via the Internet at <http://pubs.acs.org>.

OM990774S